NOTES AND CORRESPONDENCE

Data-Based Meridional Overturning Streamfunctions for the Global Ocean

LYNNE D. TALLEY, JOSEPH L. REID, AND PAUL E. ROBBINS

Scripps Institution of Oceanography, University of California, San Diego, La Jolla, California

3 April 2002 and 10 March 2003

ABSTRACT

The meridional overturning circulation for the Atlantic, Pacific, and Indian Oceans is computed from absolute geostrophic velocity estimates based on hydrographic data and from climatological Ekman transports. The Atlantic overturn includes the expected North Atlantic Deep Water formation (including Labrador Sea Water and Nordic Sea Overflow Water), with an amplitude of about 18 Sv through most of the Atlantic and an error of the order of 3–5 Sv (1 Sv $\equiv 10^6$ m^3 s^{-1}). The Lower Circumpolar Deep Water (Antarctic Bottom Water) flows north with about 8 Sv of upwelling and a southward return in the South Atlantic, and 6 Sv extending to and upwelling in the North Atlantic. The northward flow of 8 Sv in the upper layer in the Atlantic (sea surface through the Antarctic Intermediate Water) is transformed to lower density in the Tropics before losing buoyancy in the Gulf Stream and North Atlantic Current. The Pacific overturning streamfunction includes 10 Sv of Lower Circumpolar Deep Water flowing north into the South Pacific to upwell and return southward as Pacific Deep Water, and a North Pacific Intermediate Water cell of 2 Sv. The northern North Pacific has no active deep water formation at the sea surface, but in this analysis there is downwelling from the Antarctic Intermediate Water into the Pacific Deep Water, with upwelling in the Tropics. For global Southern Hemisphere overturn across 30°S, the overturning is separated into a deep and a shallow overturning cell. In the deep cell, 22–27 Sv of deep water flows southward and returns northward as bottom water. In the shallow cell, 9 Sv flows southward at low density and returns northward just above the intermediate water density. In all three oceans, the Tropics appear to dominate upwelling across isopycnals, including the migration of the deepest waters upward to the thermocline in the Indian and Pacific. Estimated diffusivities associated with this tropical upwelling are the same order of magnitude in all three oceans.

It is shown that vertically varying diffusivity associated with topography can produce deep downwelling in the absence of external buoyancy loss. The rate of such downwelling for the northern North Pacific is estimated as 2 Sv at most, which is smaller than the questionable downwelling derived from the velocity analysis.

1. Introduction

The water properties of the global ocean are determined by the large-scale, relatively slow flow of water masses from their formation regions into the deep and intermediate oceans. The flow of water away from regions of formation must be balanced by a return flow along other pathways. These circulations carry heat, freshwater, and other dissolved constituents such as components of the carbon system, oxygen, and nutrients. All the major global water masses are involved: the intermediate waters (Labrador Sea Water, North Pacific Intermediate Water, Antarctic Intermediate Water, Southeast Indian Subantarctic Mode Water, Mediterranean Water, and Red Sea Water) and the deep waters [North Atlantic Deep Water (NADW), Lower Circumpolar Deep Water or Antarctic Bottom Water, Pacific Deep Water, and Indian Deep Water]. The role of these water masses in carrying heat was explored in Talley (1999, 2003). These water masses are usually identified through their large-scale properties, especially on vertical cross sections through the ocean. The redistribution of properties by ocean currents is an integral factor in the coupled climate system and ocean ecosystems. A simplified view or diagnostic of this large-scale, cross-ocean basin circulation is often based on the zonally integrated meridional transports of mass and other properties in each ocean basin, that is, on the meridional overturning circulation.

Most quantitative depictions of this diagnostic of the global circulation are based on numerical simulations (e.g., Böning and Semtner 2001; Gent 2001; Hasumi and Suginohara 1999; Manabe and Stouffer 1993; Marotzke and Willebrand 1991; Smith et al. 2000; Weaver et al. 1998), since complete velocity analyses from top to bottom at numerous latitudes are required and dif-

Corresponding author address: Dr. Lynne D. Talley, Scripps Institution of Oceanography, University of California, San Diego, 9500 Gilman Dr., La Jolla, CA 92093-0230.
E-mail: ltalley@ucsd.edu

ficult to derive from data. Paleoclimate modelers also often diagnose major changes in circulation by examining the meridional overturn (e.g., Stocker and Schmittner 1997).

The meridional overturning streamfunction per se has thus far not been depicted based on in situ data. There are three published global velocity analyses based on absolute geostrophic velocities derived from hydrographic station data: Macdonald (1998), Ganachaud and Wunsch (2000), and Reid (1994, 1997, 2003). The first two use inverse models to solve for the unknown geostrophic reference velocities. Both provide enough information for comparison of meridional overturn with models. The Reid analyses determine the unknown geostrophic reference velocities for each hydrographic station pair, but through examination of measured geostrophic shear and tracer distributions subjected to rigorous mass balance, as in an inverse model, rather than through the algebraic formalisms of an inverse model.

Schmitz (1995, 1996) synthesized a large number of available transports based on direct current observations as well as geostrophy into a quantitatively balanced set of schematics of the global overturning circulation. Some regions, such as the Atlantic, are remarkably detailed, while others (North Pacific) are virtually devoid of information; upwelling was considered to occur somewhere but could not be localized. More global analyses are in progress, using data assimilation into numerical circulation models as well as inverse models, but are not complete.

Here we depict the meridional overturn for the three ocean basins, using a subset of the Reid (1994, 1997, 2003) circulations. The Reid circulations are a complete global analysis of geostrophic velocity, with careful attention to the adjustment of the observed geostrophic shear to match the observed property distributions on isopycnal surfaces, from top to bottom. These solutions satisfy many of the same constraints as inverse models (e.g., geostrophic shear, mass conservations, flow in congruence with tracer properties) but are found iteratively rather than in a single least squares solution. While aspects of the Reid solutions depend on subjective choices by the analyst, the same is true for the current state of inverse methods. Solutions, and associated uncertainties, from inverse methods depend critically on the choice of weight matrices that contain information regarding the assumed accuracy of the constraint equations a well as a priori estimates of errors in the initial guess of the solution. In practice, it is not possible to rigorously determine these weight matrices based on observational data. Rather, they are typically chosen based on subjective decisions of the inverse analyst or, at best, based on examination of an imperfect numerical model of the ocean. Once the weight matrices are created, the inverse method provides an ''objective'' solution but this is only with respect to the subjectively created weights. Thus, we regard the Reid absolute velocity field as equally valid, though more laboriously obtained, to inverse solutions. The strength of comparison of the results of these different methods arises from their independence and distinction of how subjective choices by the analyst are implemented.

In the analysis here, the possible importance of the Tropics for diapycnal upwelling within the large global overturning cells is apparent. Weak, broad upwelling transports are not as directly measurable as regionally confined dense water formation. The powerful early models of abyssal circulation (Stommel and Arons 1960) assumed uniform upwelling everywhere. We find that in the zonally averaged picture, much of the upwelling occurs within 20° and possibly 10° latitude of the equator. Upwelling may be restricted to an even narrower equatorial band, but is not resolved by these zonal sections. This tropical concentration of deep upwelling was previously shown by Ganachaud and Wunsch (2000).

Southern Ocean overturn south of 30°S is divided in these Reid analyses into two almost distinct downwelling cells: an upper, presumably subtropical cell with downwelling and northward subduction of surface waters into lower thermocline waters, and a larger deep downwelling cell of 22–27 Sv (1 Sv = 10^6 m^3 s^{-1}) of deep waters converted to bottom waters. Unlike Sloyan and Rintoul (2001a), we find only small upwelling from intermediate to shallow levels south of 30°S in the Southern Ocean. The magnitude of Southern Ocean overturn here is comparable to Ganachaud and Wunsch's (2000) values, which are smaller than Sloyan and Rintoul's (2001a).

We also find two large-scale features of the deep overturn that are typically not included in global syntheses—formation of Indian Deep Water in the northern Indian Ocean (Beal et al. 2003), and a surprising and perhaps incorrect downwelling in the deep northern North Pacific that is unassociated with surface buoyancy forcing. These features are presented in the spirit of showing the overturn based strictly on Reid's velocity analyses without modification.

Heat transports from the Reid (1994, 1997) Pacific and Atlantic circulation analyses were computed previously (Fig. 1), to identify the separate roles of shallow subduction in the subtropical gyres and of the deeper meridional overturning associated with intermediate and deep water formation (Talley 1999, 2003). The meridional overturning streamfunction is a straightforward by-product of that exercise and is described here, using finely divided isopycnal layers. Isopycnal layers are preferred because they illustrate the active surface buoyancy forcing and interior diffusion that must occur in order for water to change density. For comparison with most model-based streamfunctions, the overturn is also computed as a function of pressure.

Uncertainty in the diagnosed streamfunction is large, on the order of 3–5 Sv (section 2). Future global analyses using data assimilation or well-constrained global inverses may well produce more accurate streamfunc-

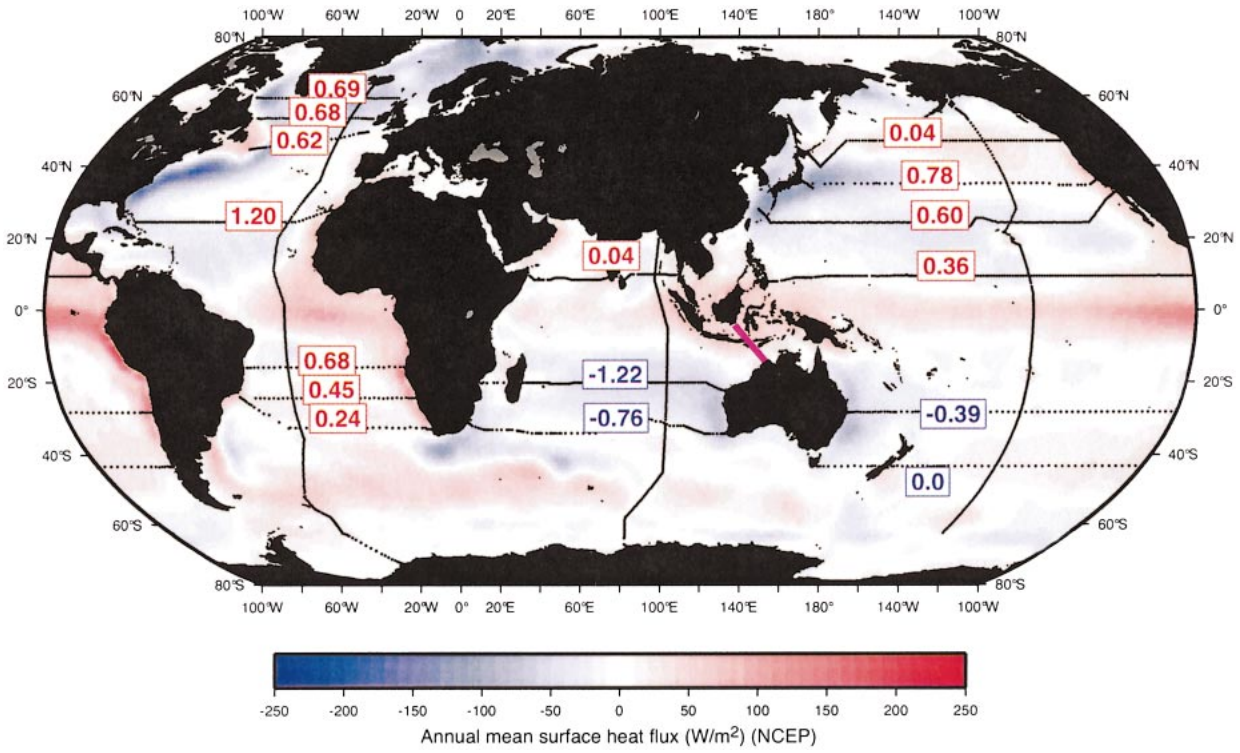

FIG. 1. Zonal hydrographic sections used for meridional overturning streamfunction, labeled with the net heat transport (PW) perpendicular to the sections, after Talley (2003), but here using NCEP winds for Ekman transports and Reid's (2003) Indian Ocean geostrophic velocities. Northward (southward) heat transports are positive (negative). Heat transports across 28°, 43°S in the Pacific and 20°, 32°S in the Indian Ocean include flux through the Indonesian archipelago, assumed to be 8 Sv at 14°C. The meridional sections in Fig. 1 are indicated.

tions. However, we feel it important to present this version of a data-based streamfunction as a comparison point for future efforts, given the present extremely small ensemble of global analyses. We are currently incorporating the North Pacific Reid (1997) velocities in an inverse model of the Pacific World Ocean Circulation Experiment (WOCE) hydrographic data to test the robustness of the deep downwelling when subjected to oxygen transport constraints and various diapycnal diffusivity assumptions. [Robbins and Bryden's (1994) inverse solution at 24°N in the Pacific was successfully constrained to include no deep downwelling, despite the deep downwelling found in Bryden et al.'s (1991) reference-level-based analysis of the same dataset.]

Presentation of ocean transports in terms of a zonally averaged streamfunction is somewhat limiting, since the lateral circulations so evident in circulation maps and transports (e.g., Reid 1994, 1997, 2003) are obscured through the layer averaging and relatively coarse layer selection. The most important missing elements are the wind-driven gyres above the thermocline, which carry a significant fraction of the heat and freshwater (Talley 2003; L. D. Talley et al. 2003, unpublished manuscript). In the deeper layers, the lateral circulations often carry Southern Hemisphere water northward and Northern Hemisphere water southward, with the net transport to the north or south just a small residual; this hemispheric property exchange is not very apparent in the zonally averaged summaries. Sloyan and Rintoul (2001b) accounted specifically for these recirculations within layers in their Southern Ocean inverse.

2. Datasets and method

Meridional (north–south) mass transport through each zonal (east–west) hydrographic section (Fig. 1) is due to geostrophic and Ekman velocities. Geostrophic velocities were calculated (Reid 1994, 1997, 2003) from hydrographic station temperature and salinity data collected over many years, from the International Geophysical Year (1957/58) to WOCE (1990s). Climate variations are small compared with the uncertainty in this geostrophic calculation, which is estimated at about 20% (Talley 2003). Ekman layer velocities were calculated using annual mean surface winds from the National Centers for Environmental Prediction (NCEP) reanalysis, and were assigned to the top 50 m (Ralph and Niiler 1999). Velocities were integrated zonally and in isopycnal layers to produce transports. The original Reid geostrophic transports balanced mass without including Ekman transport, which is especially important for heat transports given the warmth of the surface layer. Geostrophic velocities at each station pair and depth were therefore adjusted barotropically so that the total trans-

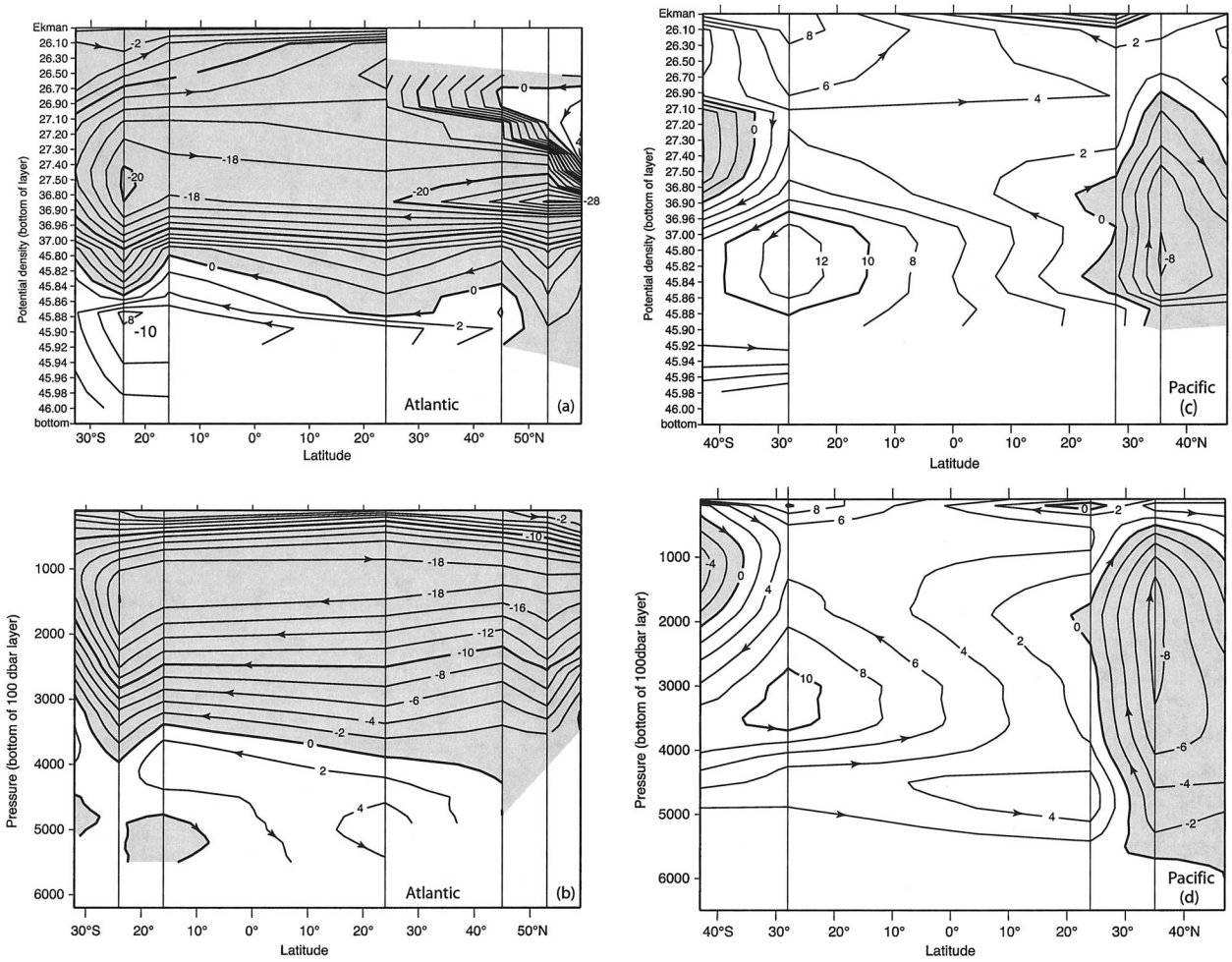

FIG. 2. Meridional overturning streamfunction (Sv) for the (a), (b) Atlantic; (c), (d) Pacific; and (e), (f) Indian Oceans, based on transports perpendicular to the zonal sections shown in Fig. 1, and using the isopycnal layers of Fig. 3. The vertical axis in (a), (c), (e) is potential density, relative to 0, 2000, and 4000 db (σ_θ, σ_2, σ_4), respectively. Section locations are shown by vertical lines and the left and right axes. Geostrophic volume transports were computed for each isopycnal layer (a), (c), (e) or for 100 db pressure layers (b), (d), (f) with the topmost layer including both the geostrophic and Ekman transport. Transports were then integrated from the ocean bottom to the top to produce the streamfunction.

port (geostrophic and Ekman) equals the transport of the original geostrophic calculation (Talley 2003).

Reid (1994, 1997) assumed that the total Atlantic (Pacific) section transports are 1.5–2.0 Sv southward (northward), due to flow from the Pacific to the Atlantic through the Bering Strait and the Arctic. The actual throughput is less [0.9 Sv from Roach et al. (1995)], but this difference has little impact on results (Talley 2003). Reid (1997, 2003) assumed an Indonesian Throughflow of 3 Sv. This is much lower than the observed 9.3 ± 2.5 Sv (Gordon et al. 1999), which itself might be too low since it is based only on Makassar Strait observations. Wind-driven transport estimates including the presence of Australia as an island also suggest higher transports (Godfrey and Golding 1981). A new throughflow experiment will start soon to measure all straits. The South Pacific and Indian sections were adjusted upward here, to include 8 Sv of throughflow using a uniform adjustment to the geostrophic velocities. A higher transport was tested in Talley (2003), but 8 Sv matches Robbins and Toole (1997), whose Indian Ocean 32°S analysis was used for heat transports in Talley (2003), which was completed prior to Reid's (2003) Indian Ocean analysis. The Robbins and Toole (1997) solution is also used here for the Southern Ocean overturn.

The overturning streamfunction for each ocean in isopycnal layers (Figs. 2a,c,e) was calculated by first computing meridional transports in isopycnal layers for each zonal section and then integrating from the ocean bottom to the top. The transport at the sea surface is equal to the net transport through the section (equal to the Bering Strait and/or Indonesian throughput on a given section). Isopycnal layers were chosen to cover the water column and water masses at the latitudes spanned by the sections (Fig. 1). Isopycnals include all of those

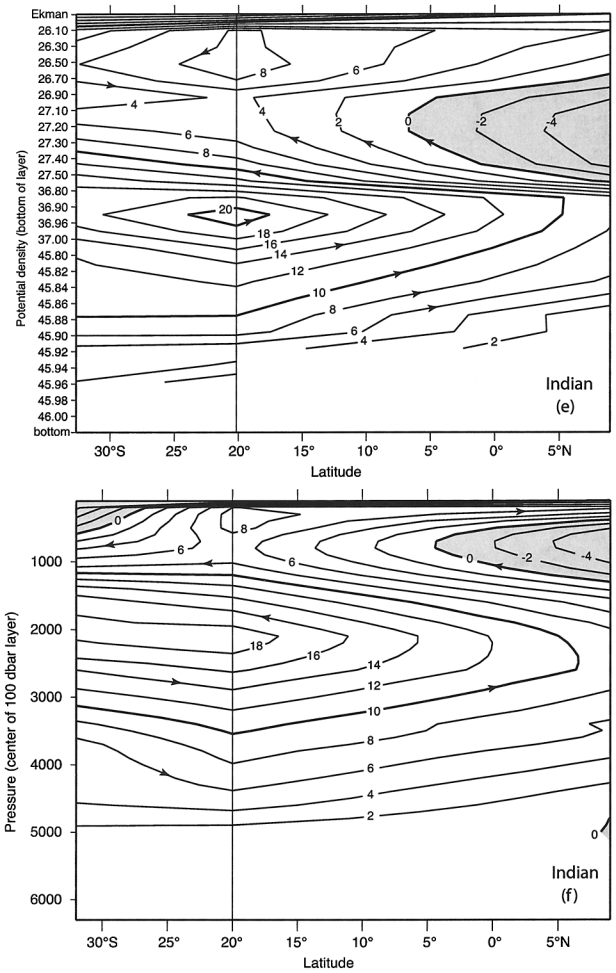

FIG. 2. (*Continued*)

shown by Talley (2003) to discriminate northward and southward transport in layers in all oceans, plus additional isopycnals for better vertical resolution. Potential densities of the isopycnal surfaces are referenced to 0, 2000, and 4000 db. The overturning streamfunction is insensitive to whether potential density or neutral density is used.

Overturning was also computed separately in pressure layers of 100-db thickness (Figs. 2b,d,f), which is a more common diagnostic than overturn in isopycnal layers. The noncoincidence of isopycnal and pressure layers results in differences in the maximum transports of overturning cells.

''Upwelling'' and ''downwelling'' refer throughout to velocity through the layer interfaces; that is, diapycnal transport for isopycnal layers and vertical transport for pressure layers.

Not all zonal sections from Reid (1994, 1997, 2003) were useful. Talley (2003) showed that several Atlantic sections yield heat transports wildly at odds with the other sections and with previous works. Indeed when these sections were included in the overturning streamfunctions, they produced an extremely noisy field. Detailed examination of transports in layers on these suspect sections shows areas where the original velocity analyses have serious problems. There are two types of incompatible sections: all tropical sections (within 15° latitude of the equator, because of the large Ekman adjustments and large geostrophic velocities and hence larger transport errors) and sections based on poorly sampled 1950s datasets or pieced from different datasets and with very large station separation. These limitations are detailed in Talley (2003) and summarized in the next paragraphs.

Tropical sections are difficult to incorporate into the global flow field because geostrophic and Ekman velocities are large and temporally variable, leading to poor signal-to-noise when computing the transports. The three tropical Atlantic sections (11°S, 8°S, and 8°N) have too much northward flow in the bottom layer as opposed to placement in the near-surface layer, thus leading to net southward heat transport on these sections and a bottom water overturn inconsistent with that farther south in the Atlantic. The tropical Pacific section at 10°N produces a reasonable heat transport since almost all of the heat is carried in a very shallow overturn in the near-surface layers (Wijffels et al. 1996), but the overturning streamfunction in the deep water is suspect by virtue of its magnitude and discontinuity with the neighboring North Pacific 24°N section. In addition to large tropical velocities, the tropical Indian Ocean sections are affected by monsoons, which create deep-reaching circulation responses (Schott et al. 1989) with current reversals documented to the ocean bottom in the Arabian Sea (Beal et al. 2000a). The Indian section at 8°S produces a heat transport that is unphysically large and a large, isolated meridional overturn and is thus suspect. The Indian Ocean sections at 9°N are used here since there is no other Northern Hemisphere information, but the results should be interpreted cautiously.

Three nontropical Atlantic sections (36°N, 32°N, and 40°S) are not included. The 32°N section is multiply nonsynoptic (pieced from datasets from 1957, 1960, and 1986). The 32°N meridional heat transport is close to 0 PW (Talley 2003), which is a diagnostic of a significant problem with the circulation. (The meridional overturning in the 32°N solution is much weaker than in the 24°N solution.) The 40°S South Atlantic section is also constructed from many cruises and is extremely sparsely sampled in midocean. It also produces heat transport near 0 PW and overturns that are inconsistent with the rest of the Atlantic. The 1981 36°N section probably could be included—its heat transport of 0.9 PW is reasonably consistent with adjacent sections and with Roemmich and Wunsch (1985) and Macdonald (1998). The NADW meridional overturn in this analysis of 36°N is about 4 Sv weaker than at 24°N, which may be a good indicator of the overall error in the streamfunctions presented here.

Uncertainty in the computed overturn is difficult to

TABLE 1. Western boundary current transport comparisons.

Location	Transports from this study [Reid (1949), (1997), (2003) adjusted geostrophic flow with additional Ekman adjustments]		Western boundary current transports from current meter arrays	
	Ship, dates, and western boundary current stations	Western boundary current transport, max pressure	Experiments, dates, and references	Western boundary current transport, and standard error, std dev, and max pressure
Atlantic 26°N	R/V *Atlantis 109*, Sep 1981, 240–250	30.0 Sv, 750 db	STACS, Apr 1982–Jun 1985, Schott et al. (1988) Lee et al. (2001)	30.5 ± 3.3 Sv, range 20–40 Sv, 750 m
Atlantic 30°S	R/V *Melville*, Nov 1972, 1–7	−23.9 Sv, 4018 db	WOCE ACM3, Jan 1991–Nov 1992, Müller et al. (1998)	−22.4 ± 2.6 Sv, 11 Sv (rms), 3208 m
Pacific 24°N	R/V *T. Washington*, Jun 1985, 370–389	29.4 Sv, 1894 db	WOCE PCM1, Sep 1994–May 1996, Lee et al. (2001)	21.5 ± 2.5 Sv, 4 Sv (rms), 927 m
Pacific 28°S	R/V *El Tanin*, July 1967, 178–185	−29.3 Sv, 4838 db	WOCE PCM3, Sep 1991–Mar 1994, Mata et al. (2000)	−22.1 ± 4.6 Sv, 30 Sv (rms), 4600 m
Indian 32°S	R/V *Darwin*, Nov 1987, 7,4,13–24	−66.7 Sv, 5164 db	WOCE ICM1, Feb 1995–Apr 1996, Bryden and Beal (2001)	−69.7 ± 21.5 Sv, 5500 m

quantify. The Reid (1994, 1997, 2003) circulation analyses have no error bars. Uncertainties could be assigned based on measurement error, and would be of the same order of magnitude as those shown by Macdonald (1998). As discussed by Rintoul and Wunsch (1991) and Robbins and Toole (1997), the actual error bars, both for our analysis and for the global inverse models, should include sensitivity to the subjective choices that lead to nonuniqueness of the solution, including initial reference velocities, layer choices, mass balance weightings, criteria for choosing the ''best'' solution (closeness to original reference velocity solution), and the importance of external constraints such as topographic cul-de-sacs. Robbins and Toole used a bootstrap method to examine sensitivity of their Indian 32°S solution to initial reference levels, from which they produced an error bar. Full evaluation of this error is not really possible without direct velocity time series in all regions. Thus, we caution against using these results too literally for comparison with model results.

Western boundary current transports at each of the subtropical sections (24°N and 30°S in all oceans) can be compared with current meter arrays (Table 1), which include means, standard errors, standard deviations, and ranges. Allowing for the slight difference in the regions covered by the hydrographic western boundary currents and the current meter arrays, as evidenced by different maximum depths, the transports are comparable. Equivalence for the Gulf Stream (North Atlantic 24°N) is not surprising since the Florida Current transport from direct observations was taken into account by Reid (1994), but the other boundary current observations had not been reported (or measured in some instances) prior to his analyses. The difference in the North Pacific's Kuroshio transport appears to be due to the restriction of the current meter array to the channel west of the Ryukyu Islands (Lee et al. 2001; note maximum depths of estimates). The difference in the East Australia Current is probably related to the very large interannual range (Mata et al. 2000). The comparison suggests that the basinwide transport balances in Reid (1994, 1997, 2003) yield reasonable mean boundary current transports, and partially validates our assumption of 3–5-Sv errors for the overturning.

Robustness of the overturns was further explored by computing the streamfunctions with the original geostrophic velocities (unadjusted for Ekman transport), and then with Ekman adjustments based on the Hellerman and Rosenstein (1983) annual mean winds instead of NCEP winds. The location and direction of major overturning circulations do not change from one version to another. Overturn strengths differ by no more than 1 Sv for the two different wind climatologies, and differ from the unadjusted original transports by up to 3 Sv, with the difference reaching 5 Sv for the NADW at 24°N in the Atlantic.

Finally, silica, freshwater, and oxygen transports were calculated from each of the sections (not shown). Silica should be almost conserved on a top-to-bottom section since any fluxes of silica into a closed region can be balanced only by deposition of silica at the ocean bottom or input from land sources. This constraint was used by Robbins and Toole (1997) for the Indian Ocean transports at 32°S, reducing to 12 Sv the earlier overturning estimate of 27 Sv using the same data (Toole and Warren 1993). Ganachaud et al.'s (2000) use of silica conservation in the Indian Ocean reduced this overturning transport even further to 11 Sv. Our oxygen and silica transports (not shown) indicate that there is likely noise on the order of 3–5 Sv in the overturning streamfunctions.

3. Meridional overturning transports

a. Atlantic Ocean (Figs. 2a,b and 3a)

The zonally averaged Atlantic overturn is dominated by the NADW (including Labrador Sea Water) and Antarctic Bottom Water cells. The NADW cell extends the length of the Atlantic, with southward transport of 18 Sv between $36.9\sigma_2$ and $45.9\sigma_4$ at most latitudes. This net southward transport is a well-known feature of the global circulation (e.g., Merz and Wüst 1922; Wüst 1935; Broecker 1991; Schmitz 1995) and corresponds with the southward-extending high-salinity core (Fig. 3a). The maximum overturn of 26 Sv at 59°N is probably an overestimate (McCartney and Talley 1984; Dickson and Brown 1994; Schmitz and McCartney 1993). Note though that in pressure layers (Fig. 2b), the maximum overturn is significantly lower, around 18 Sv. A reduction in strength to 12 Sv appears between 24° and 32°S, although this may not be significant. Northward upper-ocean flow feeds the NADW formation and is separated from the southward flow of NADW at about $27.5\sigma_\theta$. This is the maximum density usually associated with the low-salinity Antarctic Intermediate Water layer based on water mass properties (e.g., Rintoul 1991; Talley 1996).

The northward upper-ocean flow is transformed to lower density (diapycnal upwelling) in the tropical South Atlantic to the base of the thermocline at $26.3\sigma_\theta$ (based on the additional tropical sections not shown in Fig. 2). It then downwells in the major buoyancy loss region of the Gulf Stream just north of 24°N (Speer and Tziperman 1992). The southward outflow is adiabatic (unchanging density) from the northern North Atlantic to 32°S.

In the northernmost North Atlantic there is a surface cell of 2–4 Sv, with upwelling in the north and downwelling in the Gulf Stream/North Atlantic Current. This subpolar cell is due to high-latitude freshening that creates low-density flow in the East Greenland and Labrador Currents (e.g. McCartney and Talley 1984). In the subtropical gyre, 16 Sv of low density Gulf Stream waters continue on to the subpolar gyre without subducting back southward (Talley 2003). Zonal averaging and the strength of this North Atlantic overturn from surface waters to deep waters suppresses the strong, nearly lateral circulation in the uppers ocean in the subtropical gyre (13 Sv at 24°N). The associated shallow overturn (warm water poleward and cooler water equatorward near the sea surface) carries up its one-third of the North Atlantic heat-transport (Talley 2003). The near-surface subtropical gyre of about 6 Sv in the South Atlantic is also obscured by zonal averaging (represented as 2 Sv in Fig. 2a). These near-surface gyres, however, carry a significant fraction of the heat transport in both basins.

The Atlantic's bottom water cell includes northward flow of up to 8.5 Sv of the densest water [Antarctic Bottom Water (AABW), also called Lower Circumpolar Deep Water (LCDW)] with upwelling in the Tropics and North Atlantic into the bottom of the NADW. This increases the total southward ''NADW'' transport to 26 Sv at 24°S. (AABW is the lower salinity water at the ocean bottom that extends northward from the Antarctic—Fig. 3b.) The AABW disappears as a distinct water mass in the North Atlantic around the latitude of Bermuda. The dividing density between northward bottom flow and southward deep water flow is around $45.91\sigma_4$. (The weakened AABW cell of 3.8 Sv at 32°S is probably due to noise in the transport field rather than reflecting actual deep downwelling between 24° and 32°S.) Previous estimates of NADW transport southward out of the Atlantic are 17–18 Sv (Rintoul 1991; Schmitz 1995; Sloyan and Rintoul 2001a) up to 22 Sv (Holfort and Siedler 2001).

b. Pacific overturn (Figs. 2c,d and 3b)

The subtropical gyre shallow overturning in the North and South Pacific is less obscured by the zonal averaging than in the Atlantic, showing 6 (8) Sv of the 32 (24) Sv of shallow lateral circulation for the North (South) Pacific (Talley 2003). The South Pacific has an especially clear signal, given the density layers used here, reaching to the Antarctic Intermediate Water ($27.1\sigma_\theta$ and slightly greater). The 10°N section was intentionally omitted from our presentation for reasons described above, but does show the strong shallow overturn with a balance between the northward Ekman and southward near-surface geostrophic flow that is apparent in Wijffels et al. (1996). In the northern (subpolar) North Pacific, the weak North Pacific Intermediate Water (NPIW) formation cell is apparent, with a magnitude of 2.5 Sv at 47°N (density lower than $26.3\sigma_\theta$ moving northward and densities $26.3–27.2\sigma_\theta$ moving southward). This NPIW overturn is reduced to 1.5 Sv overturn at 35° and 24°N [also as in Talley (2003), and with independent information in Talley (1997) and Yasuda (1997)]. This overturn strength is comparable to estimates based on hydrographic data within the Okhotsk Sea (Gladyshev et al. 2003).

As is well known, the Pacific meridional overturn differs from the Atlantic overturn because of the absence of vigorous dense water formation in the North Pacific. In the South Pacific, the expected northward flow of LCDW (AABW) is found at densities greater than $45.86\sigma_4$, upwelling north of 28°S. The maximum transport of the LCDW cell is 13 Sv here, which is roughly equivalent to Tsimplis et al.'s (1998) 12 Sv and Wijffels et al.'s (2001) estimate of 8–9 Sv, with different layer definitions. As in the Atlantic calculation, the reduced cell strength on the southernmost section is possibly an artifact since LCDW originates in the Southern Ocean south of 43°S. This likely reflects limitations in the overall accuracy of the circulations.

There is no significant surface ventilation of deep water in the North Pacific. [A tiny amount of renewed water has been found at the bottom of the Bering Sea

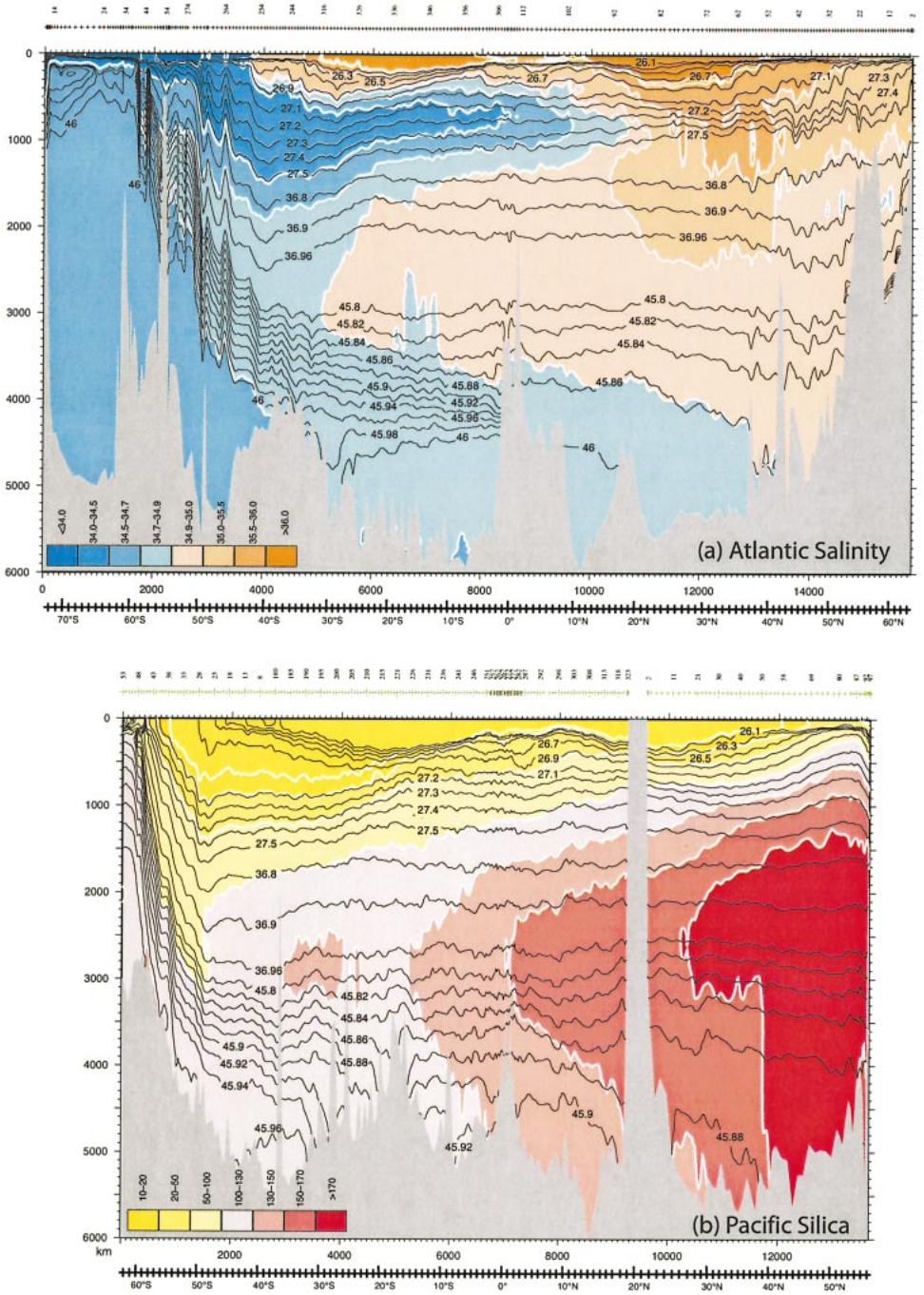

FIG. 3. (a) Meridional section of salinity in the Atlantic Ocean, along approximately 20°–25°W. (b) Meridional section of dissolved silicate (μmol kg^{-1}) in the Pacific Ocean along approximately 150°W. (c) Meridional section of salinity in the Indian Ocean along approximately 95°E. Black contours show the isopycnals bounding the layers used in the meridional overturning streamfunction (σ_θ = surface to 27.5; σ_2 = 36.80–36.96; σ_4 = 45.80–bottom). Section locations are shown in Fig. 1.

(Warner and Roden 1995) but it has not been shown to have a large-scale impact on North Pacific properties.] The densest recurring surface ventilation is in the Okhotsk Sea in the northwestern North Pacific. Direct ventilation there, through brine rejection during sea ice formation, reaches only to about 27.0σ_θ. Vigorous tidal mixing where the Okhotsk Sea exchanges with the North Pacific extends the high-oxygen and low-salinity properties of the directly ventilated waters down to 27.6σ_θ, at about 2000 db (Talley 1991).

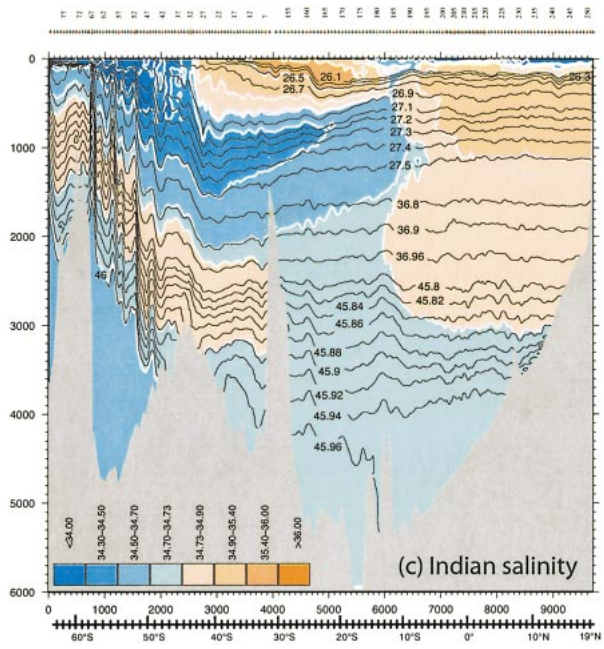

FIG. 3. (*Continued*)

The deep water overturn of the North Pacific is usually shown as upwelling of northward-flowing bottom waters (LCDW) from the South Pacific (Johnson and Toole 1993; Roemmich and McCallister 1989) into the overlying Pacific Deep Water layer, which is characterized by a middepth silicate maximum (Fig. 3b) and oxygen minimum (Kenyon 1983; Talley et al. 1991; Roemmich et al. 1991). The North Pacific deep water cell here (Figs. 2c,d) is therefore perplexing, showing 5–8 Sv of *downwelling* from the lower parts of the intermediate waters ($27.1\sigma_\theta$–$36.96\sigma_2$) into the Pacific Deep Water denser than $45.86\sigma_4$ and flowing southward toward the equator as dense water. Five Sv of this occurs in the restricted region north of 47°N. The downwelling is closed by upwelling in the Tropics. (This is a good example of the danger of overinterpreting zonally summed transports since the obvious hemispheric exchange within isopycnal layers is obliterated in the summation.) The cell is reported here because it is a consistent feature of the Reid (1997) North Pacific analysis, including the 10°N section (not shown because tropical sections were excluded from this paper).

A possible North Pacific deep downwelling cell was diagnosed but de-emphasized in the past using the same data as here [at 24°, 35°, and 47°N in Roemmich and McCallister (1989); at 24°N in Bryden et al. (1991); at 47° but not at 24°N in Macdonald (1998)]. These authors may have chosen not to discuss it (Roemmich and McCallister; Macdonald) or were suspicious of the result (Bryden et al.) because of its apparent lack of physicality, particularly if diapycnal diffusion is assumed to be constant. Robbins and Bryden (1994) looked closely at the putative downwelling at 24°N and found that they could constrain the velocities to create upwelling throughout the deep water layer. Wijffels et al. (1996) obtained deep downwelling with their initial geostrophic reference velocity choices for the 10°N section, but required its absence in their inverse solution. This issue is discussed further in section 4.

c. Indian overturn (Figs. 2e,f and 3c)

The Indian overturn based on Reid's (2003) geostrophic velocities, adjusted for Ekman transport, has both expected and some surprising elements. The northward flow of deep water into the southern Indian Ocean is a well-documented feature of the 32°S section (Toole and Warren 1993). The net northward flow is identified with both the high-salinity deep layer extending northward and the lower-salinity bottom water beneath it (Fig. 3c). This deep inflow upwells into the thermocline and above within the Indian Ocean and then returns southward (Warren 1981; Fu 1986; Toole and Warren). The 18-Sv strength of the inflow, upwelling, and overturn is within the wide range of recent estimates [7 Sv in Ganachaud et al. (2000); 12 Sv in Robbins and Toole (1997); 10 Sv in Bryden and Beal (2001); 23 Sv in Sloyan and Rintoul (2001a); 24 Sv in Schmitz (1995)]. Our 18-Sv overturn does not conserve silica. Silica conservation applied by Robbins and Toole (1997) reduced Toole and Warren's (1993) 27-Sv overturning estimate to 12 Sv. The two other lower estimates (Ganachaud et al. 2000; Bryden and Beal 2001) also conserve silica.

North of the equator in the western Indian Ocean (Arabian Sea), the evaporative Red Sea creates a thick high-salinity layer (Indian Deep Water) north of 10°S. This is laterally separated from the high-salinity water (Circumpolar Deep Water) in the southern Indian Ocean (Fig. 3c) which originates near Africa and includes a significant North Atlantic Deep Water component (Reid 2003). The lower-salinity deep water separating the two high-salinity cores is also from the Southern Ocean, but enters the Indian Ocean south of Australia and therefore has the lower-salinity characteristic of Circumpolar Deep Water of the eastern Indian Ocean (Reid and Lynn 1971; Schmitz 1995; Hufford et al. 1997; Reid 2003).

The Indian Ocean north of 32°S has two competing processes—overall upwelling that returns the deep waters originating from the south as much warmer water, and water mass formation that creates the middepth Indian Deep Water (Figs. 2e,f). The Circumpolar Deep Water (CDW) upwells in both the Tropics and at the northern boundary north of the equator. The northern section at 9°N was included in order to give a general idea of tropical and northern overturn, although the uncertainty is much greater than for any other section presented here because of its low latitude and strong monsoonal forcing. We caution that the solutions presented here that depend on this section should not be taken too literally. Recent analyses of the Arabian Sea portion of the 9°N section by Beal et al. (2000a,b, 2003), Shi et

al. (2002), and Stramma et al. (2002) are the best guides to overturning in this region. Chereskin et al. (2002) and Beal et al. (2003) indicate that the monthly Ekman transport is more appropriate than annual for this section. We thus used the monthly Ekman transport for 9°N. With this analysis, 10 Sv of CDW upwell between 20°S and 9°N while 8 Sv upwell in the northernmost regions. In the northern Indian Ocean, there is a 2-Sv upwelling near the surface that returns southward mainly as Ekman transport. There is also a downwelling of 4 Sv, creating saline Indian Deep Water. This downwelling is likely too strong, given the tiny 0.37 Sv of actual new Red Sea Water that enters the Indian Ocean (Bower et al. 2000). In Beal et al.'s (2003) inverse model of the Arabian Sea portion of the 9°N section, there is 1 Sv of Indian Deep Water formation and 4 Sv of upwelling into the Ekman layer.

In Fig. 2, Indian Deep Water formed in the north appears to upwell in the Tropics, before reaching 20°S. However, Indian Deep Water clearly penetrates southward into the Agulhas Current (Beal et al. 2000a; Bryden and Beal 2001). Northward transport of Circumpolar Deep Water overcompensates the southward Indian Deep Water transport. Thus, as noted before, the important lateral exchanges evident on isopycnals (Reid 2003) are obscured by the zonal summations.

The upper ocean in the subtropical Indian Ocean includes a subduction overturn with a maximum strength of 8 Sv, from the surface to about 26.9σ_θ, which is the density of the Southeast Indian Subantarctic Mode Water. This cell is clear and in the correct sense for subduction when depicted in terms of isopycnal layers (Fig. 2e), but does not make sense and is obscured when displayed in pressure layers (Fig. 3f), because of the bowling of isopycnals through pressure levels.

d. Southern Ocean overturn (Fig. 4)

The overturning north of 30°S from the three oceans can be examined for its implications for the Southern Ocean south of 30°S. Results were reported in Talley (2003) and are shown again here. The Robbins and Toole (1997) Indian Ocean 32°S transports were used in Talley (2003) since Reid's (2003) circulation was not available, and are preferred for our estimate (Fig. 4a) since Robbins and Toole conserved silica, resulting in a weaker Indian Ocean deep upwelling cell.

The Southern Ocean overturn consists of two apparently independent overturning cells, separated vertically at 27.0σ_θ. The deeper cell is composed of southward flow of North Atlantic and Pacific Deep Waters, transformed into much denser Lower Circumpolar Deep Water in the Antarctic and returning northward at the ocean bottom. This deep cell has a net strength of 22 Sv using the Robbins and Toole result [Fig. 4a; 27 Sv with the Reid (2003) Indian section, Fig. 4b]. The dense water formation in this cell occurs south of the Antarctic Circumpolar Current, along the Antarctic continental margins (e.g., Rintoul 1998; Orsi et al. 1999).

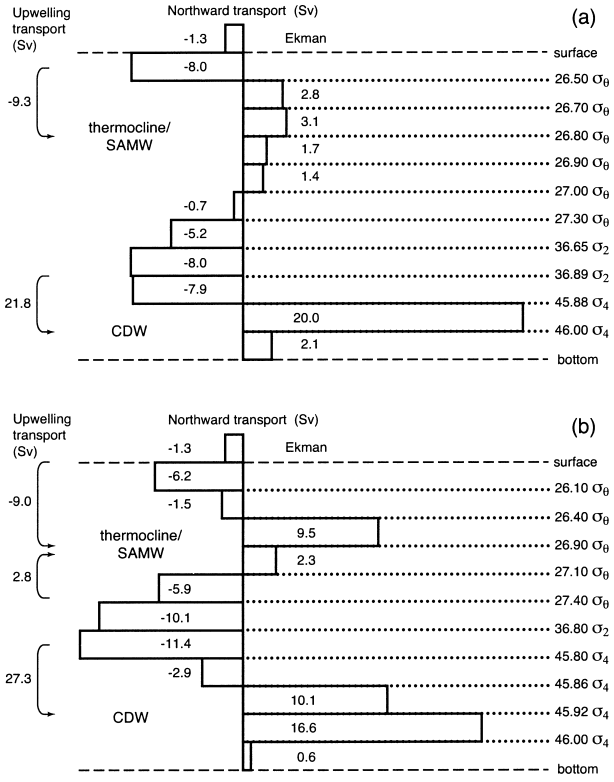

FIG. 4. Meridional overturn in coarse isopycnal layers for the Southern Ocean at approximately 30°S (28°S–Pacific; 30°S–Atlantic; 32°S–Indian). (a) From Talley (2003), using Reid's (1994, 1997) Atlantic and Pacific velocities and Robbins and Toole's (1997) Indian velocities, showing a deep overturning cell of 22 Sv of northward transport below 45.88 σ_4, formed in the Antarctic from southward flowing deep water layers. (b) The same as (a) but with Reid's (2003) Indian Ocean velocities.

The upper-ocean cell, above 27.0σ_θ, is a balance between 9 Sv of southward Ekman and surface layer transport and northward return flow of thermocline water and Subantarctic Mode Water (Fig. 4a). This upper-ocean cell is due to subtropical gyre subduction (in the three Southern Hemisphere oceans), with poleward surface layer flow and equatorward denser flow. It probably only marginally involves the Southern Ocean south of the Antarctic Circumpolar Current, as the densest waters in this upper cell originate at the sea surface north of the Antarctic Circumpolar Current. We note that Antarctic Intermediate Water (AAIW), with densities 27.0–27.5σ_θ, falls within the net southward transport in the deep water layers. This is due to the dominance of deep water upwelling in the Indian Ocean north of 30°S, which creates southward flow at the AAIW densities there (where there is no local source of AAIW). Northward transport of mass and especially freshwater in the AAIW layer in the Atlantic and Pacific is an important part of their budgets, despite the global southward transport.

TABLE 2. Estimated tropical upwelling rates, areas, velocities, and diapycnal diffusivities.

Ocean (lat band for calculation)	Upwelling transport (1×10^6 m^3 s^{-1})	Surface area 2000 m* (m^2)	Avg vertical velocity (cm s^{-1})	Diapycnal diffusivity (cm^2 s^{-1})
Atlantic (10.5°S–10.5°N)	8	1.20×10^{13}	7×10^{-5}	1.5
Atlantic (2.5°S–2.5°N)	8	0.32×10^{13}	25×10^{-5}	5.5
Pacific (10.5°S–10.5°N)	14	3.70×10^{13}	4×10^{-5}	0.8
Pacific (2.5°S–2.5°N)	14	0.88×10^{13}	16×10^{-5}	3.5
Indian (10.5°S–10.5°N)	10	1.34×10^{13}	7×10^{-5}	1.7
Indian (2.5°S–2.5°N)	10	0.33×10^{13}	31×10^{-5}	6.8
Indian (north of 8.5°N)	8	0.45×10^{13}	18×10^{-5}	3.9

* Using etopo5 bathymetry at 1° resolution to calculate areas at 2000-m depth.

The deep water cell of 22 Sv (27 Sv using Reid's Indian velocities) is comparable to Ganachaud and Wunsch's (2000) and Wijffels et al.'s (2001) estimates but smaller than Macdonald's (1998) 36 Sv, Schmitz's (1995) 48 Sv, and Sloyan and Rintoul's (2001a) 50 Sv. The differences from Schmitz are that the northward LCDW ($\sigma_4 > 45.88$) in the Pacific (Indian) is 9 (10) Sv here and 20 (24) Sv in Schmitz. For the Pacific, Schmitz quoted a range of 10–20 Sv based on a number of references, and chose the high end for the overall synthesis. Wijffels et al. (2001) also find about 16–20 Sv of LCDW inflow from the WOCE Pacific 32°S section. For the Indian, Schmitz used Toole and Warren's (1993) estimate of bottom and deep water into the Indian Ocean, which was shown by Robbins and Toole (1997) to be too large by about 15 Sv. The difference from Sloyan and Rintoul is more methodological—the circulations here are based on consistency with circulation and isopycnal properties in the ocean basins north of 30°S, while Sloyan and Rintoul constrain their estimates with air–sea fluxes south of 30°S.

A significant difference from Sloyan and Rintoul (2001a) is that there is very little upwelling of deep water into the thermocline waters here. There is none if the Robbins and Toole (1997) Indian 32°S transport is used, and 3 Sv if the Reid (2003) transport is used, which could be zero given the errors.

4. Discussion

Global deep water cells dominate the overturning zonally averaged circulations of the three oceans. The North Atlantic Deep Water overturn of about 18 Sv at maximum compares well with numerous previous estimates based on geostrophic velocities and also direct velocity measurements. The Antarctic provides an equivalent Southern Hemisphere deep water cell of about 22 Sv, which may be somewhat too small, compared with other analyses. Intermediate water cells are weaker than the deep water cells. Shallow overturns in the subtropical gyres (Talley 2003) are obscured in these zonally averaged transports because they occur in much narrower density layers than used here.

Diapycnal upwelling in the Tropics is a major factor in the overturning cells shown here and in Ganachaud and Wunsch (2000). In the Atlantic, the northward-flowing upper-ocean water from the South Atlantic upwells significantly in the Tropics before becoming denser through surface heat loss in the Gulf Stream region; approximately 8 Sv are involved (Fig. 2a; Table 2). In the Pacific and Indian Oceans, deep water also mainly upwells in the Tropics, separating Northern and Southern Hemisphere deep water circulations. The tropical Indian deep upwelling (Fig. 2e) consists of about 12 Sv of southern source Circumpolar Deep Water in the denser part of the water column and 8 Sv of the northern source Indian Deep Water in the upper-water column, so we take the average tropical upwelling rate as 10 Sv. The Pacific upwelling transport is about 14 Sv (Fig. 2b).

Diapycnal velocity (transport/area) is estimated in Table 2 for two different assumptions of latitude range for tropical upwelling [a 2.5°S–2.5°N band or a 10.5°S–10.5°N band, using earth topography–5 min (etopo5) bathymetry on a 1° grid], since our hydrographic estimates cannot localize it within this band. The diapycnal diffusivity κ is estimated from this vertical velocity with the average vertical density structure used in Robbins and Toole (1997). Diapycnal diffusivities estimated for the upwelling velocities estimated here are 1–2 cm^2 s^{-1} for the Tropics if upwelling is within 10° of the equator and 3–7 cm^2 s^{-1} if upwelling occurs within 2.5° of the equator. Previous estimates of diapycnal diffusivity required for the Indian Ocean budgets have fluctuated from being much larger than in other oceans (Toole and Warren 1993) to about the same size as elsewhere (Robbins and Toole 1997). However, since the tropical upwelling rate obtained here for the Indian Ocean is similar to that for the Pacific and Atlantic, the diffusivities are similar.

In the Indian Ocean north of 9°N, an additional 8 Sv of Circumpolar Deep Water upwells in our adjusted Reid (2003) circulation (Fig. 2). This yields a diapycnal velocity of 1.8×10^{-4} cm s^{-1} and a slightly enhanced diapycnal diffusivity of 3.9 cm^2 s^{-1}. Error in these numbers is likely to be especially large. Half of this section lies in the Arabian Sea, which has been the subject of inverse modeling, carefully taking into account the major monsoonal current reversals (Beal et al. 2003). They obtain only 0.8-Sv upwelling through 2200 m, much smaller than in the circulation used here.

The deep downwelling diagnosed here for the northern North Pacific is puzzling since there is no surface source of dense water. One possibility is that the downwelling is present, but there is also an undiagnosed upwelling cell beneath it, which would provide the necessary bottom boundary properties that could allow the coexistence of a deep downwelling and the observed bottom properties. Another possibility is that it is simply an artifact arising from the use of a single hydrographic transect to represent a long-term mean. We present the results as is because we consider it important to diagnose these overturnings without modifiying the basic circulations (Reid 1994, 1997, 2003). We note that the observed geostrophic shear on all of these sections does not easily lend itself to a thoroughly different outcome, as described above in section 3b. D. Stammer (2002, personal communication) has also obtained a weak, deep downwelling cell in initial global data assimilation runs.

Physically, downwelling can occur without a local source of buoyancy if diapycnal diffusivity increases toward the bottom, as is observed in numerous locations, especially over rough topography (Polzin et al. 1997). The steady-state temperature equation, neglecting horizontal variations, and including variable vertical diffusivity κ is

$$w\frac{\partial T}{\partial z} = \frac{\partial}{\partial z}\left[\kappa(z)\frac{\partial T}{\partial z}\right] \quad \text{or} \tag{1a}$$

$$w = \frac{\partial \kappa}{\partial z} + \kappa\frac{\partial^2 T}{\partial z^2}\left(\frac{\partial T}{\partial z}\right)^{-1} \tag{1b}$$

The second term is positive in the deep ocean, but the first term is negative. If a vertical diffusivity of 100 $cm^2\ s^{-1}$ is assumed at the ocean bottom, decaying upward to 0.1 $cm^2\ s^{-1}$ at 100 db above the bottom, and if it is assumed that such a bottom layer exists along the 7000-km northern boundary of the North Pacific over a depth of 2 km, (1b) suggests a maximum net downward transport of 1–2 Sv, if the second term is neglected. This is smaller than the estimate here (Fig. 2c). Additionally, downwelling into a deep water layer without any underlying denser water is inconsistent with deep property distributions, as it is not possible to simply make deep water colder and more oxygenated. [The only bottom buoyancy source in the North Pacific is weak geothermal heating (Joyce et al. 1986) and oxygen is always consumed within the abyssal water column]. Therefore we suggest that while depth-dependent diapycnal diffusivity could contribute to downwelling, there must also be an underlying upwelling cell, with net northward flow of the densest, coldest bottom water.

Dense bottom water with southern properties is found in the very deep trench at the western and northern boundary of the subpolar North Pacific (Kenyon 1983; Warren and Owens 1988; Talley et al. 1991; Talley and Joyce 1992), suggesting at least some northward transport. In the Reid (1997) analysis, there is no net northward transport of this bottom water. Direct current measurements east of Japan and south of the Aleutians (Warren and Owens 1988; Kawasaki and Kono 1993; Hallock and Teague 1996) show a complex current structure near the trench, with probable northward flow seaward of the trench and southward flow along the western/northern boundary. These strong boundary currents, modified by topography and powerful transient eddies present near the western boundary, may have obscured the direction of net transport. Another possibility is that the flow is not in steady state; a 1999 reoccupation of the 47°N section shows warming in the bottom layer consistent with geothermal heating and no inflow of cold water from the south (M. Fukasawa 2001, personal communication), and so the 1985 data-set might accurately depict a present lack of a deep water source. Datasets will continue to be collected and analyzed in the North Pacific. If the deep water cell is shown to be robust, then the processes that create it could also be active in the North Atlantic and Circumpolar Deep Water overturning cells, enhancing the direct ventilation and gravity-dependent entrainment of these water masses.

Acknowledgments. This databased calculation was inspired by the WOCE numerical modeling workshop of August 1998 (thanks to J. Willebrand) and was presented at several WOCE workshops. The work was supported by National Science Foundation grants for the World Ocean Circulation Experiment: Pacific OCE-9712209, Atlantic OCE-9529584, and Indian OCE-0118046.

REFERENCES

Beal, L. M., A. Ffield, and A. L. Gordon, 2000a: Spreading of Red Sea overflow waters in the Indian Ocean. *J. Geophys. Res.,* **105,** 8549–8564.

——, R. L. Molinari, T. K. Chereskin, and P. E. Robbins, 2000b: Reversing bottom circulation in the Somali Basin. *Geophys. Res. Lett.,* **27,** 2565–2568.

——, T. K. Chereskin, H. L. Bryden, and A. Ffield, 2003: Variability of water properties, heat and salt fluxes in the Arabian Sea, between the onset and wane of the 1995 southwest monsoon. *Deep-Sea Res.,* **50,** 2049–2076.

Böning, C. W., and A. J. Semtner, 2001: High-resolution modelling of the thermohaline and wind-driven circulation. *Ocean Circulation and Climate,* G. Siedler and J. Church, Eds., International Geophysics Series, Vol. 77, Academic Press, 59–78.

Bower, A. S., H. D. Hunt, and J. F. Price, 2000: Character and dynamics of the Red Sea and Persian Gulf outflows. *J. Geophys. Res.,* **105,** 6387–6414.

Broecker, W. S., 1991: The great ocean conveyor. *Oceanography,* **4,** 79–89.

Bryden, H. L., and L. M. Beal, 2001: Role of the Agulhas Current in Indian Ocean circulation and associated heat and freshwater fluxes. *Deep-Sea Res.,* **48,** 1821–1845.

——, D. H. Roemmich, and J. A. Church, 1991: Ocean heat transport across 24°N in the Pacific. *Deep-Sea Res.,* **38,** 297–324.

Chereskin, T. K., W. D. Wilson, and L. M. Beal, 2002: The Ekman heat and salt transports at 8°30′N in the Arabian Sea during the 1995 southwest monsoon. *Deep-Sea Res.,* **49,** 1211–1230.

Dickson, R. R., and J. Brown, 1994: The production of North At-

lantic Deep Water: Sources, rates, pathways. *J. Geophys. Res.*, **99,** 12 319–12 341.
Fu., L.-L., 1986: Mass, heat and freshwater fluxes in the South Indian Ocean. *J. Phys. Oceanogr.*, **16,** 1683–1693.
Ganachaud, A., and C. Wunsch, 2000: Improved estimates of global ocean circulation, heat transport and mixing from hydrographic data. *Nature,* **408,** 453–457.
——, ——, J. Marotzke, and J. Toole, 2000: Meridional overturning and large-scale circulation of the Indian Ocean. *J. Geophys. Res.*, **105** (11), 26 117–26 134.
Gent, P. R., 2001: Will the North Atlantic Ocean thermohaline circulation weaken during the 21st century? *Geophys. Res. Lett.*, **28,** 1023–1026.
Gladyshev, S., L. Talley, G. Kantakov, G. Khen, and M. Wakatsuchi, 2003: Distribution, formation and seasonal variability of Okhotsk Sea Mode Water. *J. Geophys. Res.*, **108,** 3186, doi: 10.1029/2001JC000877.
Godfrey, J. S., and T. J. Golding, 1981: The Sverdrup relation in the Indian Ocean, and the effect of Pacific–Indian Ocean through flow on Indian Ocean circulation and on the east Australian Current. *J. Phys. Oceanogr.*, **11,** 771–779.
Gordon, A. L., R. D. Susanto, and A. Ffield, 1999: Throughflow within Makassar Strait. *Geophys. Res., Lett.*, **26,** 3325–3328.
Hallock, Z. R., and W. J. Teague, 1996: Evidence for a North Pacific Deep Western Boundary Current. *J. Geophys. Res.*, **101,** 6617–6624.
Hasumi, H., and N. Suginohara, 1999: Atlantic deep circulation controlled by heating in the Southern Ocean. *Geophys. Res., Lett.*, **26,** 1873–1876.
Hellerman, S., and M. Rosenstein, 1983: Normal monthly wind stress over the world ocean with error estimates. *J. Phys. Oceanogr.*, **13,** 1093–1104.
Holfort, J., and G. Siedler, 2001: The meridional oceanic transports of heat and nutrients in the South Atlantic. *J. Phys. Oceanogr.*, **31,** 5–29.
Hufford, G. E., M. S. McCartney, and K. A. Donohue, 1997: Northern boundary currents and adjacent recirculations off southwestern Australia. *Geophys. Res. Lett.*, **24,** 2797–2800.
Johnson, G. C., and J. M. Toole, 1993: Flow of deep and bottom waters in the Pacific at 10°N. *Deep-Sea Res.*, **40,** 371–394.
Joyce, T. M., B. A. Warren, and L. D. Talley, 1986: The geothermal heating of the abyssal subarctic Pacific Ocean. *Deep-Sea Res.*, **33,** 1003–1015.
Kawasaki, Y., and T. Kono, 1993: Results of current measurements southeast of Kushiro. *Extended Abstracts, Nemuro Workshop on Western Subarctic Circulation '93,* Nemuro, Japan, PICES (North Pacific Marine Science Organization).
Kenyon, K. E., 1983: Sections along 35°N in the Pacific. *Deep-Sea Res.*, **30,** 349–369.
Lee, T. N., W. E. Johns, C.-T. Liu, D. Zhang, R. Zantopp, and Y. Yang, 2001: Mean transport and seasonal cycle of the Kuroshio east of Taiwan with comparison to the Florida Current. *J. Geophys. Res.*, **106,** 22 143–22 158.
Macdonald, A. M., 1998: The global ocean circulation: A hydrographic estimate and regional analysis. *Progress in Oceanography,* Vol. 41, Pergamon, 281–382.
Manabe, S., and R. J. Stouffer, 1993: Century-scale effects of increased atmospheric CO_2 on the ocean–atmosphere system. *Nature,* **364,** 215–218.
Marotzke, J., and J. Willebrand, 1991: Multiple equilibria of the global thermohaline circulation. *J. Phys. Oceanogr.*, **21,** 1372–1385.
Mata, M. M., M. Tomczak, S. Wijffels, and J. A. Church, 2000: East Australian Current volume transports at 30°S: Estimates from the World Ocean Circulation Experiment hydrographic sections PR11/P6 and PCM3 current meter array. *J. Geophys. Res.*, **105,** 28 509–28 526.
McCartney, M. S., and L. D. Talley, 1984: Warm water to cold water conversion in the northern North Atlantic Ocean. *J. Phys. Oceanogr.*, **14,** 922–935.
Merz, A., and G. Wüst, 1922: Die Atlantische Vertikalzirkulation. *Z. Ges. Erdkunde Berlin,* **1,** 1–34.
Müller, T. J., Y. Ikeda, N. Zangenberg, and L. V. Nonato, 1998: Direct measurements of western boundary currents off Brazil between 20°S and 28°S. *J. Geophys. Res.*, **103,** 5429–5438.
Orsi, A. H., G. C. Johnson, and J. L. Bullister, 1999: Circulation, mixing, and production of Antarctic Bottom Water. *Progress in Oceanography,* Vol. 43, Pergamon, 55–109.
Polzin, K. L., J. M. Toole, J. R. Ledwell, and R. W. Schmitt, 1997: Spatial variability of turbulent mixing in the abyssal ocean. *Science,* **276,** 93–96.
Ralph, E. A., and P. P. Niiler, 1999: Wind-driven currents in the tropical Pacific. *J. Phys. Oceanogr.*, **29,** 2121–2129.
Reid, J. L., 1994: On the total geostrophic circulation of the North Atlantic Ocean: Flow patterns, tracers and transports. *Progress in Oceanography,* Vol. 33, Pergamon, 1–92.
——, 1997: On the total geostrophic circulation of the Pacific Ocean: Flow patterns, tracers and transports. *Progress in Oceanography,* Vol. 39, Pergamon, 263–352.
——, 2003: On the total geostrophic circulation of the Indian Ocean: Flow patterns, tracers and transports. *Progress in Oceanography,* Vol. 56, Pergamon, 137–186.
——, and R. J. Lynn, 1971: On the influence of the Norwegian-Greenland and Weddell Seas upon the bottom waters of the Indian and Pacific Oceans. *Deep-Sea Res.*, **18,** 1063–1088.
Rintoul, S. R., 1991: South Atlantic interbasin exchange. *J. Geophys. Res.*, **96,** 2675–2692.
——, 1998: On the origin and influence of Adelie land bottom water. *Ocean, Ice and Atmosphere: Interactions at the Antarctic Continental Margin,* S. Jacobs and R. Weiss, Eds., Antarctic Research Series, Vol. 75, Amer. Geophys. Union, 151–171.
——, and C. Wunsch, 1991: Mass, heat, oxygen and nutrient fluxes and budgets in the North Atlantic Ocean. *Deep-Sea Res.*, **38** (Suppl.), S355–S377.
Roach, A. T., K. Aagaard, C. H. Pease, S. A. Salo, T. Weingartner, V. Pavlov, and M. Kulakov, 1995: Direct measurements of transport and water properties through the Bering Strait. *J. Geophys. Res.*, **100,** 18 443–18 457.
Robbins, P. E., and H. L. Bryden, 1994: Direct observations of advective nutrient and oxygen fluxes at 24°N in the Pacific Ocean. *Deep-Sea Res.*, **41,** 143–168.
——, and J. M. Toole, 1997: The dissolved silica budget as a constraint on the meridional overturning circulation of the Indian Ocean. *Deep-Sea Res.*, **44,** 879–906.
Roemmich, D., and C. Wunsch, 1985: Two transAtlantic sections: Meridional circulation and heat flux in the subtropical North Atlantic Ocean. *Deep-Sea Res.*, **32,** 619–664.
——, and T. McCallister, 1989: Large scale circulation of the North Pacific Ocean. *Progress in Oceanography,* Vol. 22, Pergamon, 171–204.
——, T. McCallister, and J. Swift, 1991: A transPacific hydrographic section along latitude 24°N—The distribution of properties in the subtropical gyre. *Deep-Sea Res.*, **38,** S1–S20.
Schmitz, W. J., 1995: On the interbasin-scale thermohaline circulation. *Rev. Geophys.*, **33,** 151–173.
——, 1996: On the world ocean circulation: Volume II, The Pacific and Indian oceans/A global update. Woods Hole Oceanographic Institution Tech. Rep. WHOI-96-08, 237 pp.
——, and M. S. McCartney, 1993: On the North Atlantic circulation. *Rev. Geophys.*, **31,** 29–49.
Schott, F., T. N. Lee, and R. Zantopp, 1988: Variability of structure and transport of the Florida Current in the period range of days to seasonal. *J. Phys. Oceanogr.*, **18,** 1209–1230.
——, J. C. Swallow, and M. Fieux, 1989: Deep currents underneath the Somali Current. *Deep-Sea Res.*, **36,** 1191–1199.
Shi, W., J. M. Morrison, and H. L. Bryden, 2002: Water, heat and freshwater flux out of the northern Indian Ocean in September–October 1995. *Deep-Sea Res.*, **49,** 1231–1252.
Sloyan, B. M., and S. R. Rintoul, 2001a: The Southern Ocean limb

of the global deep overturning circulation. *J. Phys. Oceanogr.,* **31,** 143–173.

——, and ——, 2001b: Circulation, renewal, and modification of Antarctic mode and intermediate water. *J. Phys. Oceanogr.,* **31,** 1005–1030.

Smith, L. T., E. P. Chassignet, and R. Bleck, 2000: The impact of lateral boundary conditions and horizontal resolution on North Atlantic water mass transformations and pathways in an isopycnic coordinate ocean model. *J. Phys. Oceanogr.,* **30,** 137–159.

Speer, K., and E. Tziperman, 1992: Rates of water mass formation in the North Atlantic Ocean. *J. Phys. Oceanogr.,* **22,** 93–104.

Stocker, T. F., and A. Schmittner, 1997: Influence of CO_2 emission rates on the stability of the thermohaline circulation. *Nature,* **388,** 862–865.

Stommel, H., and A. B. Arons, 1960: On the abyssal circulation of the world ocean—I. Stationary planetary flow patterns on a sphere. *Deep-Sea Res.,* **6,** 140–154.

Stramma, L., P. Brandt, F. Schott, D. Quadfasel, and J. Fischer, 2002: Winter and summer monsoon water mass, heat and freshwater transport changes in the Arabian Sea near 8°N. *Deep-Sea Res.,* **49,** 1173–1195.

Talley, L. D., 1991: An Okhotsk Sea water anomaly: Implications for sub-thermocline ventilation in the North Pacific. *Deep-Sea Res.,* **38,** S171–S190.

——, 1996: Antarctic Intermediate Water in the South Atlantic. *The South Atlantic: Present and Past Circulation,* G. Wefer et al., Eds., Springer-Verlag, 219–238.

——, 1997: North Pacific intermediate water transports in the mixed water region. *J. Phys. Oceanogr.,* **27,** 1795–1803.

——, 1999: Some aspects of ocean heat transport by the shallow, intermediate and deep overturning circulations. *Mechanisms of Global Climate Change at Millenial Time Scales, Geophys. Monogr.,* No. 112, Amer. Geophys. Union, 1–22.

——, 2003: Shallow, intermediate and deep overturning components of the global heat budget. *J. Phys. Oceanogr.,* **33,** 530–560.

——, and T. M. Joyce, 1992: The double silica maximum in the North Pacific. *J. Geophys. Res.,* **97,** 5465–5480.

——, ——, and R. A. deSzoeke, 1991: Trans-Pacific sections at 47°N and 152°W: Distribution of properties in the subpolar gyre. *Deep-Sea Res.,* **38,** S63–S82.

Toole, J. M., and B. A. Warren, 1993: A hydrographic section across the subtropical South Indian Ocean. *Deep-Sea Res.,* **40,** 1973–2019.

Tsimplis, M. N., S. Bacon, and H. L. Bryden, 1998: The circulation of the subtropical South Pacific derived from hydrographic data. *J. Geophys. Res.,* **103,** 21 443–21 468.

Warner, M. J., and G. I. Roden, 1995: Chlorofluorocarbon evidence for recent ventilation of the Deep Bering Sea. *Nature,* **373,** 409–412.

Warren, B. A., 1981: TransIndian hydrographic section at Lat. 18°S: Property distributions and circulation in the South Indian Ocean. *Deep-Sea Res.,* **28,** 759–788.

——, and W. B. Owens, 1988: Deep currents in the central subarctic Pacific Ocean. *J. Phys. Oceanogr.,* **18,** 529–551.

Weaver, A. J., A. F. Fanning, M. Eby, and E. C. Wiebe, 1998: The climate of the last glacial maximum in a coupled ocean GCM/Energy-moisture balance atmosphere model. *Nature,* **394,** 847–853.

Wijffels, S. E., J. M. Toole, H. L. Bryden, F. A. Fine, W. J. Jenkins, and J. L. Bullister, 1996: The water masses and circulation at 10°N in the Pacific. *Deep-Sea Res.,* **43,** 501–544.

——, ——, and R. Davis, 2001: Revisiting the South Pacific subtropical circulation: A synthesis of World Ocean Circulation Experiment observations along 32°S. *J. Geophys. Res.,* **106,** 19 481–19 513.

Wüst, G., 1935: The Stratosphere of the Atlantic Ocean. *Scientific Results of the German Atlantic Expedition of the Research Vessel ''Meteor'' 1925–27.* Vol. 6, 109–288. (English translation, W. J. Emery, Ed., Amerind, 1978.)

Yasuda, I., 1997: The origin of the North Pacific Intermediate Water. *J. Geophys. Res.,* **102,** 893–909.